atmosphere

MDPI

# Supplementary Materials: The Air and Viruses We Breathe: Assessing the Effect the $PM_{2.5}$ Air Pollutant has on the Burden of COVID-19

**Sherrie L. Kelly [1,2,*], Andrew J. Shattock [1,2], Martina S. Ragettli [1,2], Danielle Vienneau [1,2], Ana M. Vicedo-Cabrera [3,4], Kees de Hoogh [1,2]**

**Contents**

## 1.Supplementary methods

### *1.1. Model overview*

OpenCOVID is a stochastic, individual-based transmission model of SARS-CoV2 transmission and COVID-19 disease. The model tracks individual characteristics such as age, comorbidity risk, SARS-CoV-2 infection status, COVID-19 disease state, level of immunity, and vaccination and treatment status. OpenCOVID captures the individuals' probability of viral transmission based on person-to-person contact, viral variant profile, and effect of seasonality, as well as the age-dependent probability of progressing from severe to critical disease, or eventually to death, which is heavily influenced by viral variant profile.

Open access source code for the OpenCOVID model is publicly available at https://github.com/SwissTPH/OpenCOVID. Model code is freely available for use or modification, including further or independent development.

OpenCOVID is written primarily in the R programming language (1) and is stable with R version 4.1.0. The model is being run on sciCORE (http://scicore.unibas.ch/) the scientific computing core facility at the University of Basel.

### *1.2. SARS-CoV-2 infection*

As susceptible and infectious people come into contact, if the susceptible person becomes infected with SARS-CoV-2, the model captures the individual viral transmission as a function of time since infection (Figure S1). Any contact between infectious and susceptible individuals, represented through a one-year age bin structured network (Figure S2), is assumed to carry the same probability of transmission, all else being equal. As shown in Figure S2, younger people have more contacts with the 10 to 20 year age group having the highest number of contacts. The probability of transmission is dependent on the viral load of the infectious individual, the profile of the viral variant being transmitted, and any partial immunity acquired by the susceptible individual (through previous infection and/or vaccination). Furthermore, seasonality affects the probability of transmission (see Section 1.7 *Seasonality*) with lower probabilities in warmer periods reflecting a larger proportion of people coming into contact outdoors where the probability of transmission is lower.

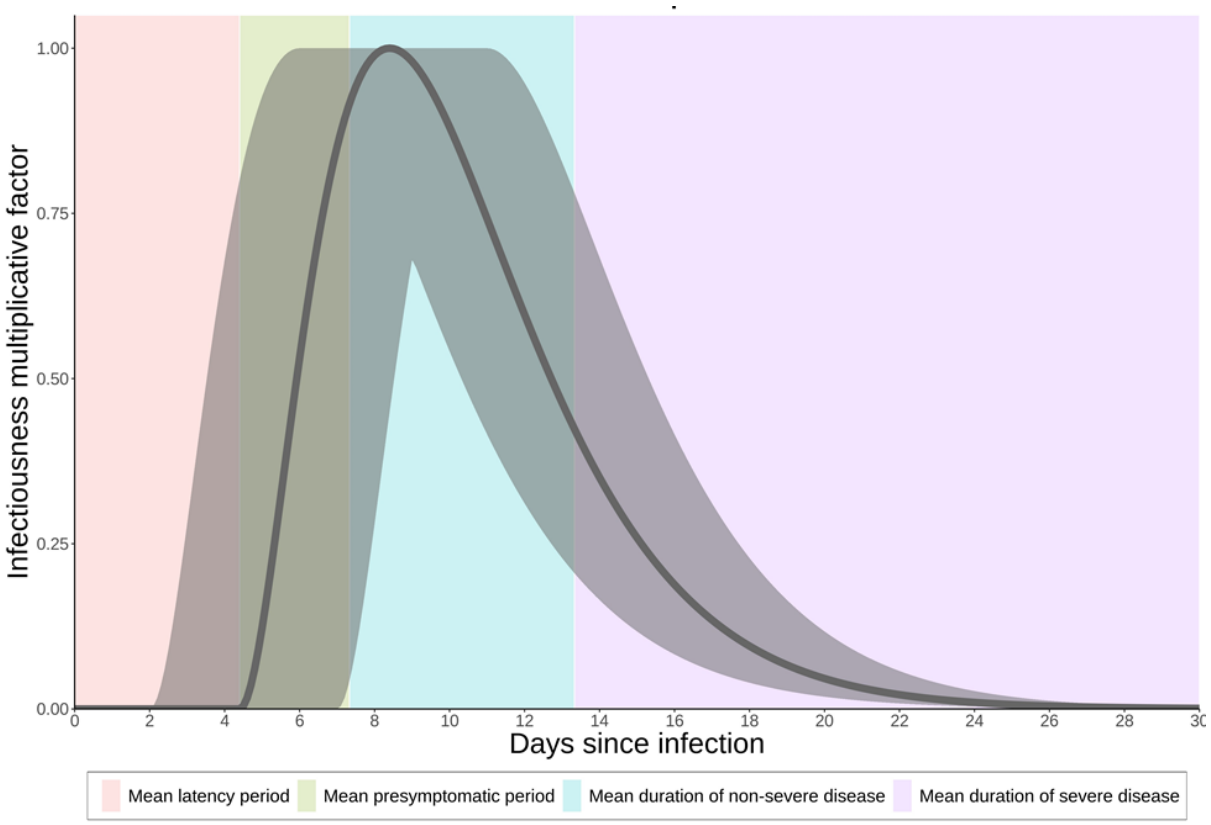


**Figure S1.** Viral load profile in OpenCOVID. The curve is standardised to between zero and one to yield an infectiousness multiplier used to calculate the probability of transmission. Peak infectivity is reached between days 6 and 14 following infection.

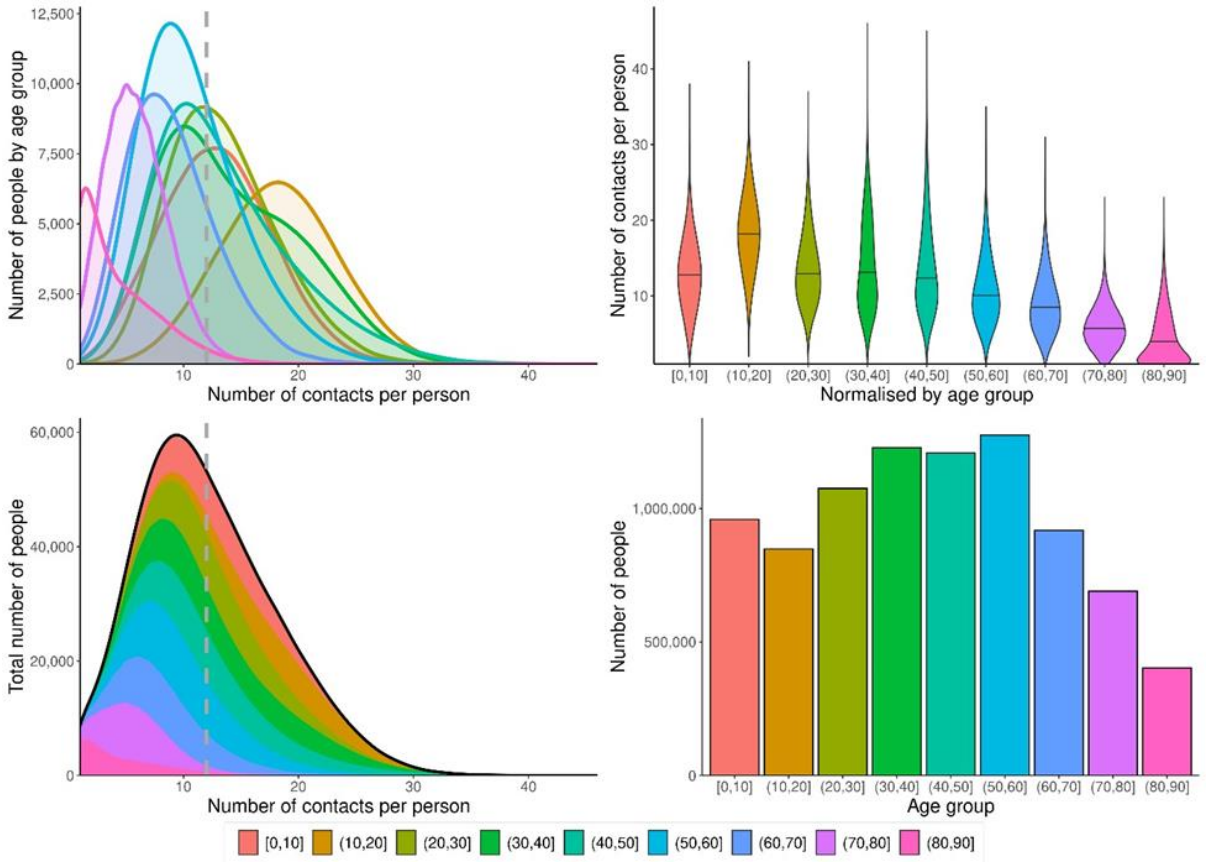

**Figure S2.** Age-related contact properties in OpenCOVID. Numbers of people by age group versus number of contacts per person (top left) show both groups' population sizes and distribution of contacts. Plots illustrate the number of contacts per person normalised by age group (top right), total number of people versus number of contacts per person (bottom left), and number of people versus age group show distribution by age group (bottom right).

*1.3. Viral transmission*

We define a pairwise transmissible contact to be a person-to-person interaction that has a transmission probability of $\beta$ when the infectious individual is fully infectious, and the susceptible individual is fully susceptible. An individual is fully infectious when their viral load is at a maximum (see Section 1.2 *SARS-CoV-2 infection*). An individual is considered to be fully susceptible when they have zero immunity (see Section 1.6 *Immunity to infection*). Two additional factors can alter the probability of transmission between an infectious individual and a susceptible individual. First, a seasonality effect reduces the probability of transmission in warmer periods, reflecting a larger proportion of contacts being outdoors with warmer temperatures (see Section 1.7 *Seasonality*). Second, novel viral variants can enter the population, being more (or less) infectious than the current dominant variant, and therefore increase (or decrease) the probability of transmission (see Section 1.4 *Viral variants*).

In equation form, the probability of transmission between an infection individual, *I*, and a susceptible individual, *S*, is given by:

$$\mathrm{P(transmission)} = \beta \cdot \nu_I(\tau) \cdot \phi_I \cdot \sigma(\tau) \cdot (1 - \mu_S(\tau)) \qquad (1)$$

Where:

- $\nu_I(\tau)$ denotes the viral load of the infectious individual at time $\tau$ (see Section 1.2 *SARS-CoV-2 infection*),
- $\phi_I$ denotes the infectivity factor of the viral variant with which the infectious individual is infected (see Section 1.4 *Viral variants*),
- $\sigma(\tau)$ denotes the seasonality scaler at time $\tau$ (see Section 1.7 *Seasonality*), and
- $\mu_S(\tau)$ denotes the immunity of the susceptible individual at time $\tau$ (see Section 1.6 *Immunity to infection*).

*1.4. Viral variants*

OpenCOVID tracks transmission chains of viral variants. The model can consider any number of variants, providing there is sufficient data to inform the relative prevalence of each variant in the population. The model is calibrated to variant prevalence over time. Each variant is assessed by assigning them a percentage increase in the probability of transmission per contact, then further calculations are conducted to capture the likely transmission advantage in a heterogeneous population with pre-existing immunity (see Section 1.6 *Immunity to infection*) during an ongoing pandemic considering the impact of any transmission control measures. We estimated the effective reproductive number, Re, of a given variant over a given period using the mean number of contacts an individual has determined by the model calibration (see Section 5.2 *Model fitting*), for the specified increase in the transmission probability. The transmission advantage is therefore the proportional increase in the expected number of cases from one infected individual in the epidemic setting in a given setting over a given period of time (including the effects of pre-existing natural immunity and the impact of control measures).

*1.5. Viral load*

During the latent period that follows infection, we assume viral load is zero (and therefore that the infected person is not yet infectious). We then use a gamma probability density function with shape parameter $\alpha = 3$ and rate parameter $\beta = 0.5$ to represent individual-level viral load over the course of the infectious period. We assume infectiousness is proportional to this viral load (2), and therefore standardise viral load values to between

zero and one to convert viral load into an infectiousness scaler that scales the probability that the individual can infect other contacts. The parameters of the gamma function were selected to best represent the current understanding of viral load profiles from time since infection (3, 4). Figure S1 illustrates this infectiousness scaler (multiplier) profile from the time since infection.

In equation form, the infectiousness scaler for an individual $k$ infected $\tau$ days after infection is given by:

$$\upsilon(\tau) = \begin{cases} 0, \tau < l \\ \upsilon'(\tau), x \geq l \end{cases} \quad (2)$$

Where $l$ is the sampled latent period for individual $k$ (see Section 2.2 *Disease state duration*) for duration distributions and

$$\upsilon'(\tau) = \frac{\beta^{\alpha}(\tau - l)^{\alpha-1}e^{-\beta(\tau-1)}}{(\alpha - 1)!} \quad (3)$$

*1.6. Immunity to infection*

SARS-CoV-2 infection/transmission and COVID-19 symptom blocking immunity can occur through naturally acquired immunity following SARS-CoV-2 infection or induced through COVID-19 vaccination (Figure S3). All forms of immunity are assumed to wane over time with the risk of new infection depending on the probability of exposure and properties of existing and potential novel SARS-COV-2 variants (i.e., infectiousness, severity, and immune evading profile). Following administration of each booster dose, vaccine-induced immunity is assumed to immediately peak at 85% (5) before exponentially waning to 15% with a half-life of 105 days (based on longer-term waning for dose 2 from (6)). For vaccine induced immunity, the infection-blocking component of the vaccine was assumed to represent 80% of the overall 85% vaccine efficacy, with the remaining 5% attributed to preventing infections from progressing to severe disease. Vaccine protection is modelled in the context of naturally acquired immunity following SARS-CoV-2 infection, whereby natural immunity is assumed to reach peak immunity of 95% aligned with findings from Chivese and colleagues (7). Before waning exponentially to 20% in 600 days (8).

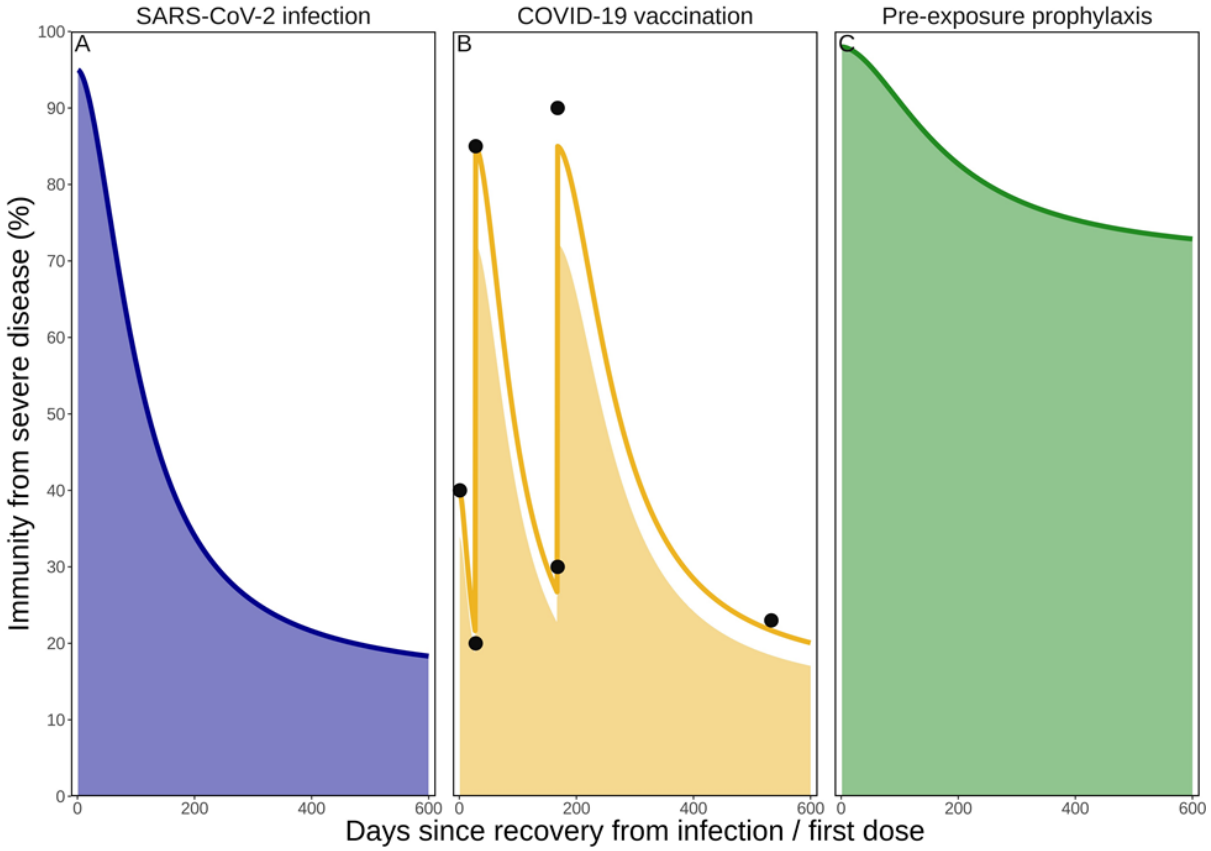


**Figure S3.** COVID-19 vaccine immunity profiles. Modelled profiles for COVID-19 vaccine induced immunity (panel A), naturally acquired immunity following infection with SARS-CoV-2 (panel B), and immunity following pre-exposure prophylaxis (panel C) are illustrated. Points shown in panel B indicate initial vaccine efficacy following primary vaccination (dose one and two) with exponential decay, with a rebound in efficacy from subsequent booster doses followed by identical exponential decay based on (6).

### *1.7. Seasonality*

Seasonality affects the probability of transmission as illustrated in Figure S4, with the grey curve representing the population-weighted best estimate for transmission probability. Daily maximum temperatures for a given setting are used and seasonality is assumed to follow a cosine function. The seasonality effect is derived from the normalised inverse of the temperature curve. This represents a reduced probability of transmission during warmer periods, reflecting a larger proportion of people coming into contact outdoors where the probability of transmission is lower, and an increased transmission probability during cooler periods, reflecting a larger proportion of contacts being in closer contact indoors where the probability of transmission is higher. A seasonality scaler, $\sigma$, is applied as a multiplicative factor in the transmission equation to reflect the effect of temperature on transmission probability per contact.

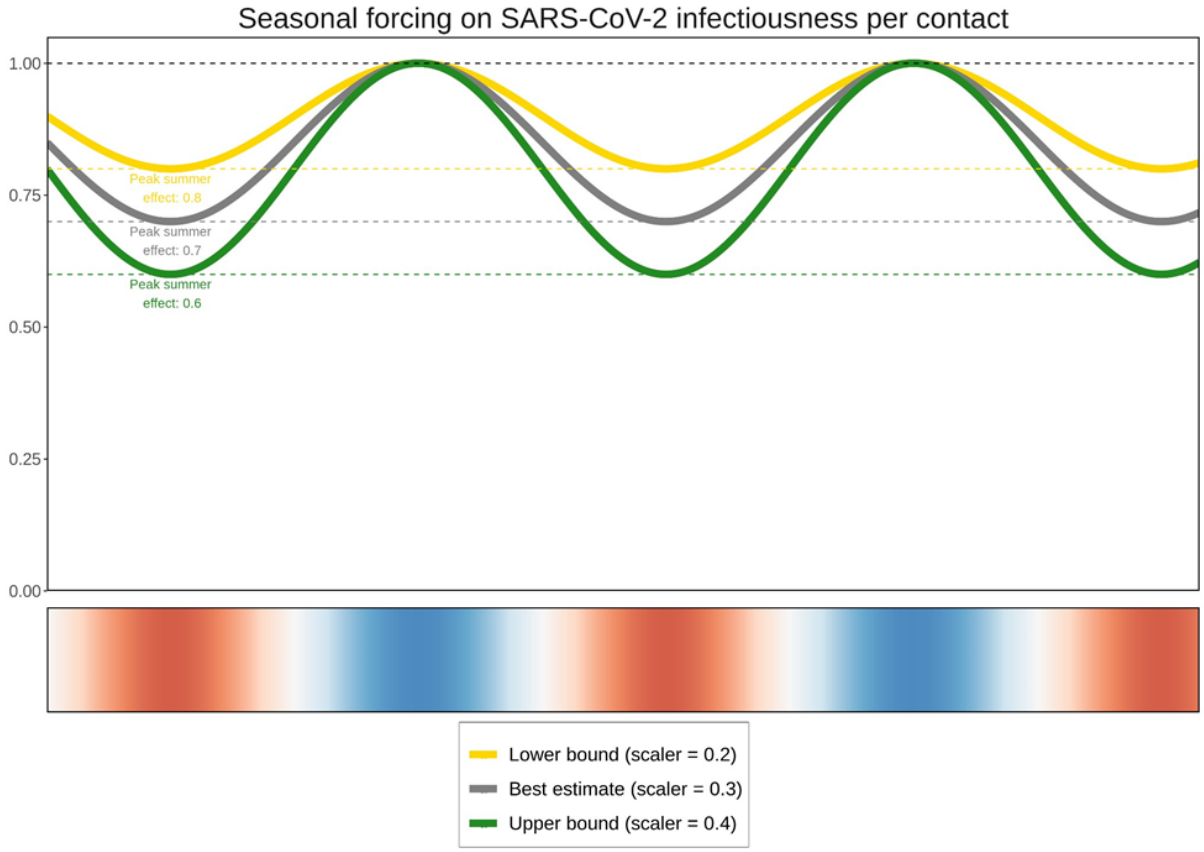


**Figure S4.** Impact of seasonal forcing scalers on SARS-CoV-2 infectiousness per contact over a two year period. The best estimate (grey curve), lower bound (yellow curve), and upper bound (green curve) from the OpenCOVID model are illustrated. Seasonality is illustrated in the bottom row where red shading indicates the warmer spring and summer seasons, blue the cooler fall and winter seasons, and white the seasonal transition periods.

### *1.8. Importation*

100 cases were imported from outside the study geographic area (i.e., cases with a travel history). The number of daily cases imported and timing of imported cases is captured in the model. There was a 5-day delay between the time of first case importation and the first confirmed case.

## 2. COVID-19 disease

### *2.1. Disease state progression*

A newly infected individual will, following a latent period, be assigned through stochastic distributions an age-dependent prognosis of either asymptomatic, mild, severe, critical disease, or eventual death (Figure S5).

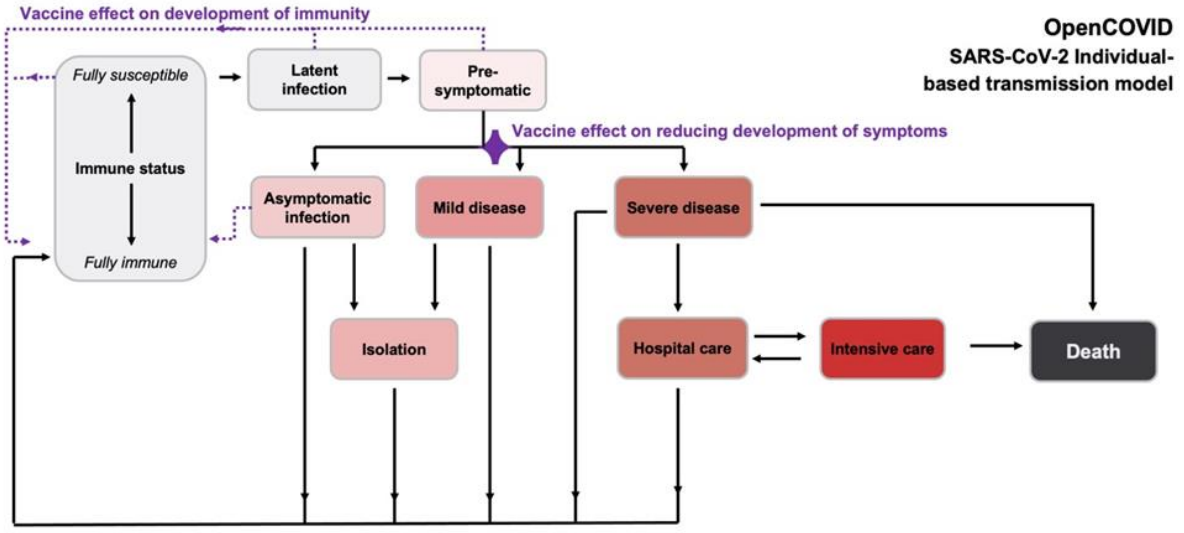


**Figure S5.** Simplified schematic of the OpenCOVID model structure. The model captures potential states of individuals. The 'immune status' ranges from fully susceptible to fully immune, where any level of immunity is a consequence of previously acquired natural immunity and/or vaccination. Development of immunity is one of the two vaccination effects modelled (indicated by dotted purple lines). Other states include latent infection, pre-symptomatic, and the asymptomatic state from which vaccination may also lead to development of immunity. After infection, some remain asymptomatic, while for others either mild or severe disease progression may occur. The second vaccine effect reduces symptom development (indicated by the purple diamond) as well as potential downstream events (isolation, hospital care, intensive care, and death). Isolation or care (hospital care, intensive care) may be required for those with symptomatic infection, resting in recovery or death. Increasingly darker shading (grey, pink, red, dark grey) indicates increasing severity.

### *2.2. Disease state duration*

Upon infection, the duration for which an individual will remain in each disease or care state is sampled from a distribution, as illustrated in Figure S6, and described in Table S1 of (9) including sources for the best estimated values for each duration.

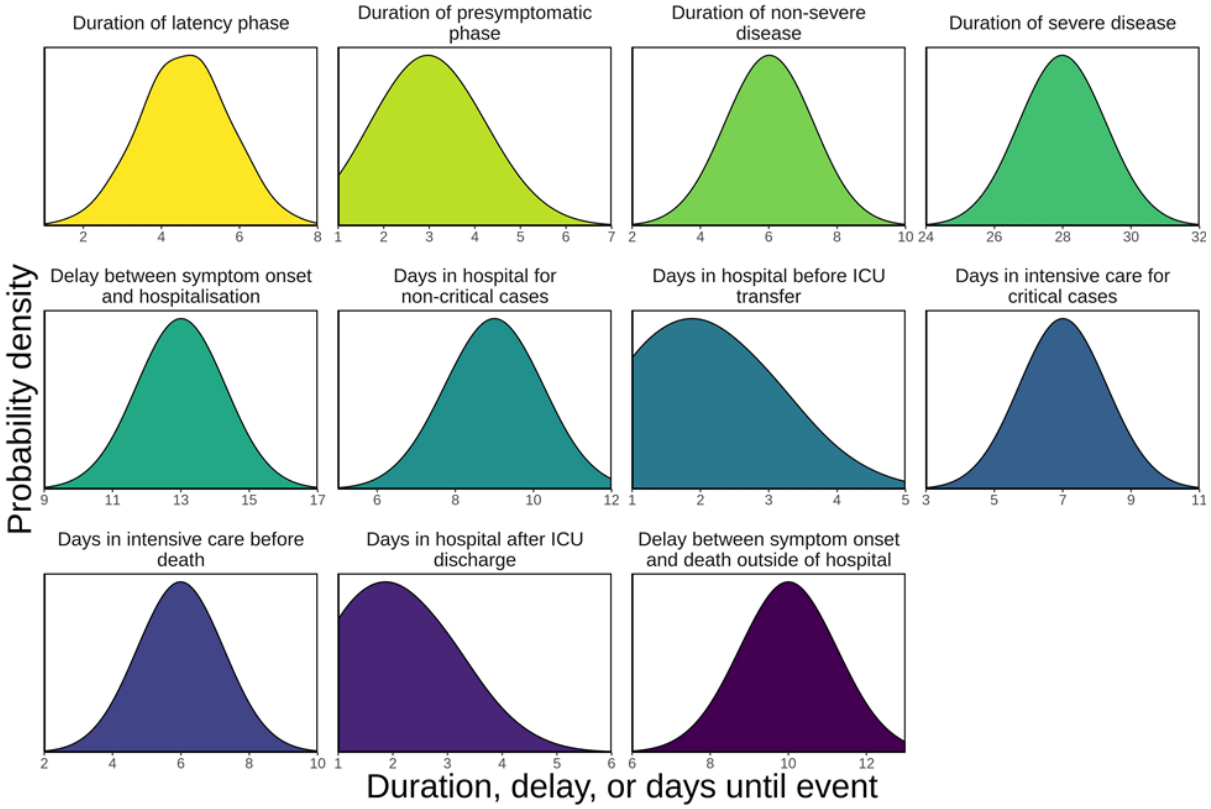


**Figure S6.** Default durations for infection latency, disease state, and hospitalisation used the in OpenCOVID model.

*2.3. Prognosis probabilities*

Once infected with SARS-CoV-2 and following a latent period, an infected individual is either asymptomatic or will develop mild or severe disease. Individuals that develop severe disease may, after some time, either seek hospital care or remain outside the hospital setting (e.g., within care homes). Three distinct prognosis tracks are modelled for those that will seek hospital care: 1) the patient will eventually recover without intensive care, 2) the patient will require intensive care but will eventually recover, and 3) the patient will require intensive care and will ultimately die from COVID-19-related complications. See Figure S6 for an illustration of the modelled natural history and prognosis pathways.

The prognosis probabilities provided in Table S1 assume an equal probability of infection across all age groups. Whilst the probability of infection in any given contact is not assumed to be age-dependent, the number of contacts for any given person is age-dependent (Figure S2). Therefore, each age-dependent prognosis probability needs to be scaled by an age-correction factor to convert to per-infection probabilities as illustrated in Figure S7. Three additional factors can affect these age-related prognosis probabilities:

1. Improved care procedures
2. Increased mortality of viral variant with which an individual is infected
3. Symptom reducing effect of vaccination

We quantified age-group stratified probabilities for each prognosis (Table S1) using age-disaggregated morbidity and mortality data from international sources (10, 11). Once infected, a prognosis is derived for all individuals by stochastically sampling from a uniform distribution.

**Table S1.** Prognosis probabilities by age, following infection with the SARS-CoV-2 Omicron varia.nt

| Age group (years) | Asymptomatic | Mild disease | Severe disease | Critical disease | Death |
|---|---|---|---|---|---|
| 0–>10 | 33.00% | 67.00% | <0.01% | <0.01% | <0.01% |
| 10–>20 | 33.00% | 66.98% | 0.02% | <0.01% | <0.01% |
| 20–>30 | 32.97% | 66.81% | 0.21% | 0.01% | <0.01% |
| 30–>40 | 32.94% | 66.52% | 0.51% | 0.03% | <0.01% |
| 40–>50 | 32.65% | 64.35% | 2.77% | 0.24% | <0.01% |
| 50–>60 | 31.73% | 58.00% | 8.91% | 1.36% | 0.01% |
| 60–>70 | 29.54% | 45.44% | 18.89% | 5.99% | 0.14% |
| 70–>80 | 26.74% | 33.23% | 22.64% | 15.21% | 2.17% |
| 80–90+ | 24.22% | 24.94% | 15.66% | 21.55% | 13.63% |

The viral variant an individual is infected with can alter age-related prognosis probabilities, capturing the ability of certain variants (known as variant severity) to cause increased morbidity and/or mortality (12).

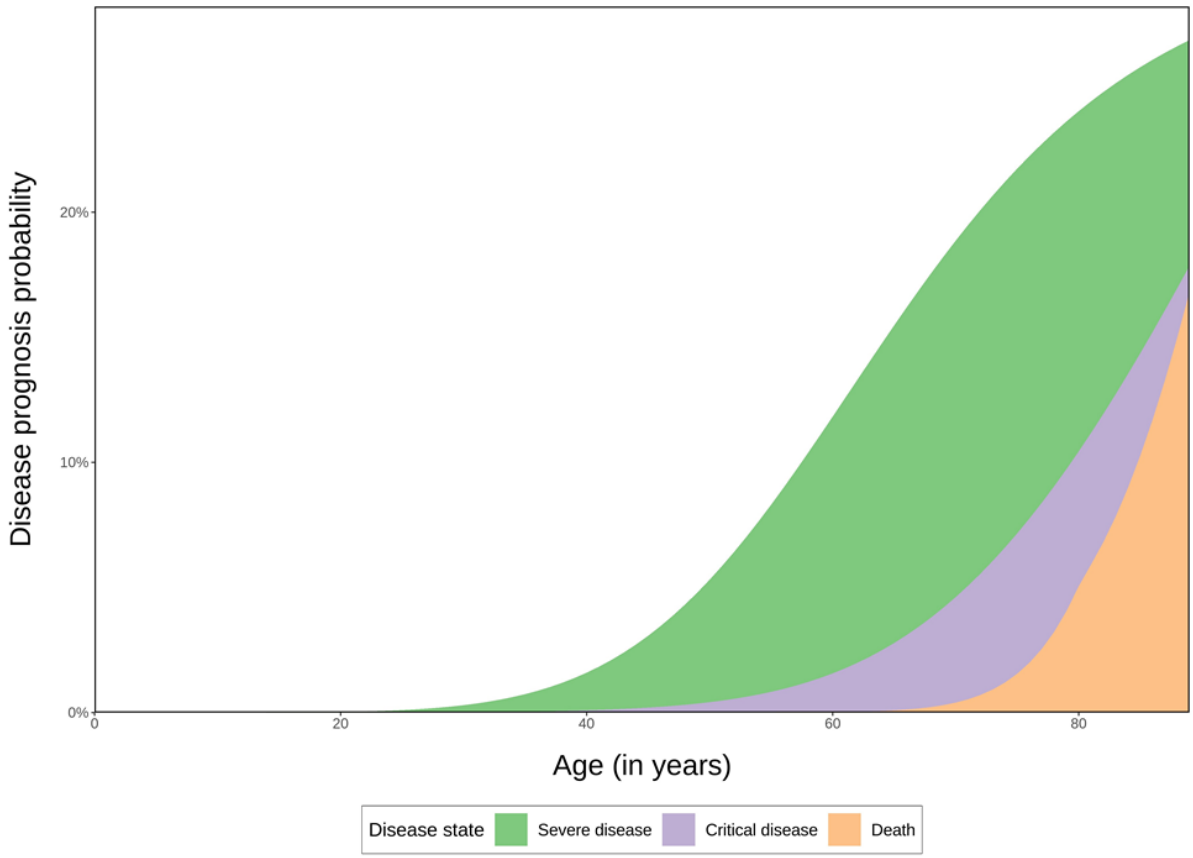


**Figure S7.** Default distributions of disease prognosis probability by age in OpenCOVID.

SARS-CoV-2 infections will result in a certain proportion of COVID-19 hospitalisations based on assumed prognosis probabilities (Table S1), and the protective effect of immunity from previous infection or vaccination are modelled to only prevent 5% of hospitalisations, but will be protective against ICU admissions and COVID-19 deaths as shown in Supplementary Information Figure S8 showing the impact of vaccine doses by variant per infections experienced by disease state (severe, critical) or death.

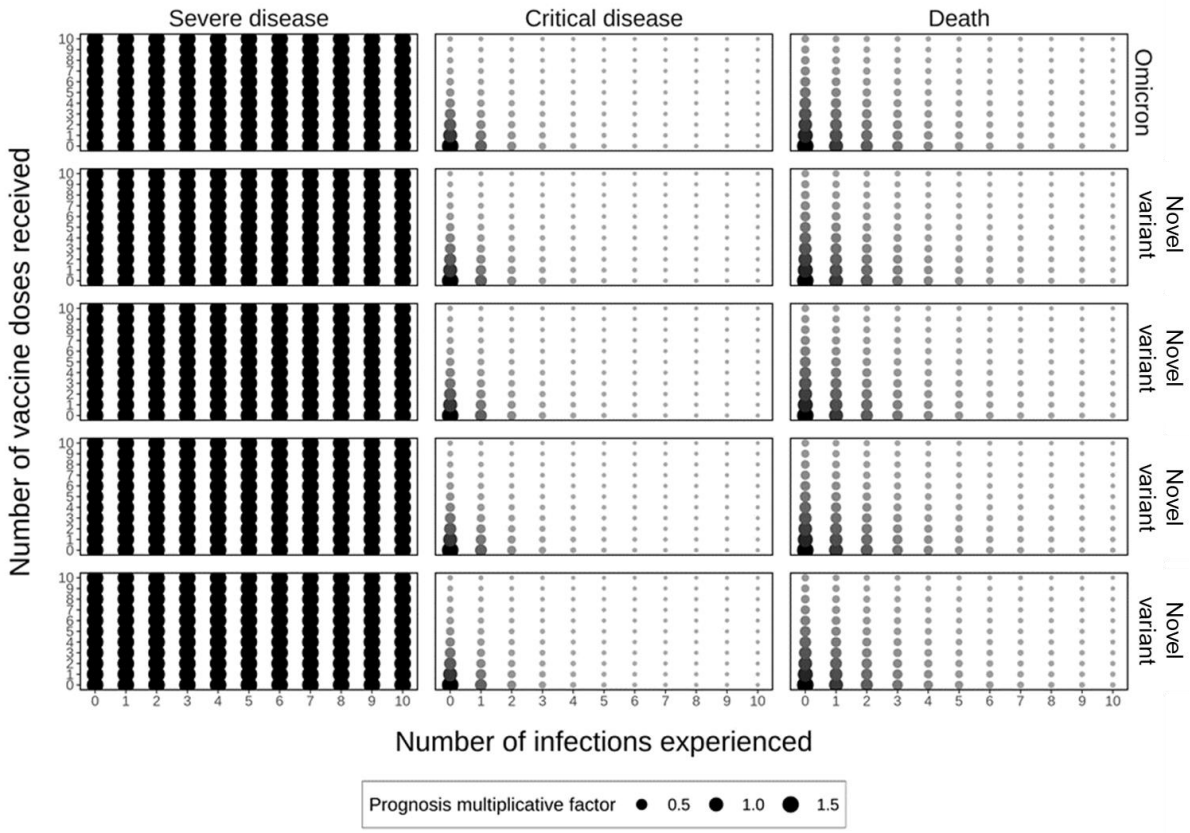


**Figure S8.** SARS-CoV-2 infections experiences per vaccine doses received. Number of COVID-19 vaccine doses received (0 to 10) per number of infections experienced (0 to 10) by disease state (severe, critical) or death for the Omicron (top row) or newly emerged (novel) SARS-CoV-2 variant (rows 2 to 4) by prognosis multiplicative factor.

*2.4. Hospital admissions*

Cases with prognosis of severe or critical disease may be admitted to hospital following some delay from symptom onset or may alternatively receive care outside of hospital (e.g., in a long-term care home). Critical cases who are in hospital will be admitted to an intensive care unit (ICU), with sufficient capacity assumed in the model. The duration an individual remains in any given disease and/or care state is sampled from a distribution (see Section 2.2 *Disease state durations*).

*2.5. Immunity*

For individuals that recover from SARS-CoV-2, we assume a partial acquired immunity of 83% to future infection upon recovery regardless of disease severity, risk group, or age (13-15).

## 3. Population

*3.1. Age and gender*

Individual ages are tracked for 0 to 90 years of age in one-year age bins, with one additional group for those aged 90 and over. The population ages each year on predefined birth dates. Gender is not considered in the model (16).

### *3.2. Contact network*

The contact network in OpenCOVID is based on the POLYMOD contact survey (17) which reports age-structured contact frequencies. The POLYMOD survey is implemented in OpenCOVID via the R package *socialmixr* (18) which provides symmetric matrices in which the rows and columns are the age class of the ego (the person reporting the contact) and the alter (the person receiving the contact), and the cell content is the average number of contacts between those age classes. This data can be accessed by country or setting. We used contact frequencies based on survey data from France, Germany, and Italy. Setting specific or archetypal age-structured demographic data were then used to sample this contact frequency space and create an age-structured random network by sampling with replacement, weighted by the average number of contacts per cell. We sample such that the resulting network has a mean number of contacts as defined by the 'contacts' parameters (see Table S1 from (9)). In such a network, not all age classes have the same number of contacts. Younger age classes have more contacts and especially have more contacts with other young age classes while older age classes have fewer contacts (Figure S2). This network does not distinguish between work, school, or home networks but is rather integrated across all these separate networks.

With beta set at a fixed value, the population average number of contacts can then be calibrated such that observed epidemiological data is matched. The primary signal for the contacts parameter is the exponential increase in all observed metrics during a given wave prior to the observed impact of any control measures.

### *3.3. Risk groups*

Risk groups include those with comorbidities with risk increasing with increasing age. Those most at risk of succumbing to COVID-19-related death are those aged 70-79 and 80 years and older.

### *3.4. Priority groups*

Priority groups represent the prioritisation for receiving a vaccination based on age groups by risk. OpenCOVID vaccinates people strictly according to their priority group, with the highest priority group receiving all doses until the target coverage is reached. Vaccine coverage can be specified by priority group for each vaccine dose.

## 4. Interventions

### *4.1. Testing, diagnosis, and isolation*

Upon infection, an individual is assigned a date at which they may potentially seek a test and be diagnosed as a confirmed COVID-19 case. The delay between symptom onset and a potential diagnosis for each individual is sampled from a truncated Gaussian distribution. By definition, all COVID-19 cases that seek hospital care receive a diagnosis. After taking hospitalised diagnoses into account, other individuals with severe disease outside of the hospital setting and individuals with mild disease are randomly selected as those who seek testing and are assigned a diagnosis in the model. To represent future test-seeking behaviour, the model calculated proportion of cases diagnosed per infected case over the past 14-days is fixed into the future. We note here that this assumption is not robust to major changes in testing policies or behaviours, including, but not limited to, mass testing. We assume no change in behaviour for individuals who test negative, and further assume that all non-severe cases isolate for a 10-day period immediately following diagnosis.

*4.2. Vaccination*

In OpenCOVID non-pharmaceutical interventions (NPIs) can curb the spread of SARS-CoV-2 by reducing the number of potentially transmissible pairwise contacts. Such measures may include the closing of non-essential shops, restrictions on mass gatherings, and facemask mandates in publicly accessible spaces. We do not explicitly simulate the effect of individual measures, but instead model the total effect of all NPIs in place.

*4.3. Treatment*

Individuals are only eligible for treatment if they have been diagnosed with a SARS-CoV-2 infection. A five-day delay between infection and diagnosis and between diagnosis and treatment initiation was modelled. Treatment can be targeted at any disease stage, those with mild symptoms not in hospital, those with severe symptoms in hospital, and those in critical condition admitted to an intensive care unit (ICU). Treatment coverage can be differentiated by priority group. We assume a certain treatment efficacy to reduce the risk of hospitalisation or death. Treatment efficacy represents the proportion who will be successfully treated in the model. Those successfully treated return to the recovered stage and are once more susceptible to infection. We assume the immunity of a person who has been successfully treated is the same as that for a person who naturally recovered. This may not be fully representative but was modelled accordingly for simplicity.

**5. Model parameters and model fitting**

*5.1. Model parameters*

See Table S1 from (9).

*5.2. Model fitting*

Using an average number of daily contacts the model was fitted to an initial effective reproduction number, $R_e$, of 1.15 at the start of the simulation period. This represents a global trend of case numbers for a dominant Omicron variant. This inherently captures the effect of any non-pharmaceutical interventions that were in place at that time, such as masking. To reflect the element of chance that naturally occurs in model transmission dynamics, 200 random stochastic simulations were performed for each scenario with 95% prediction intervals presented.

**6. Impact of $PM_{2.5}$ exposure**

*6.1. Scenario design*

The impact of a 1 to 5 μg/m$^3$ increase in average annual exposure to particulate matter ≤2.5 microns in diameter ($PM_{2.5}$) was modelled with either a 13% [95% CI 8−17%] increase in susceptibility to SARS-CoV-2 infection (19) or an 11% [95% CI 6−17%] increase in severity of COVID-19 disease (20). $Log_{10}$ and linear and relationships between these two associations were as modelled as shown in Figure S9.

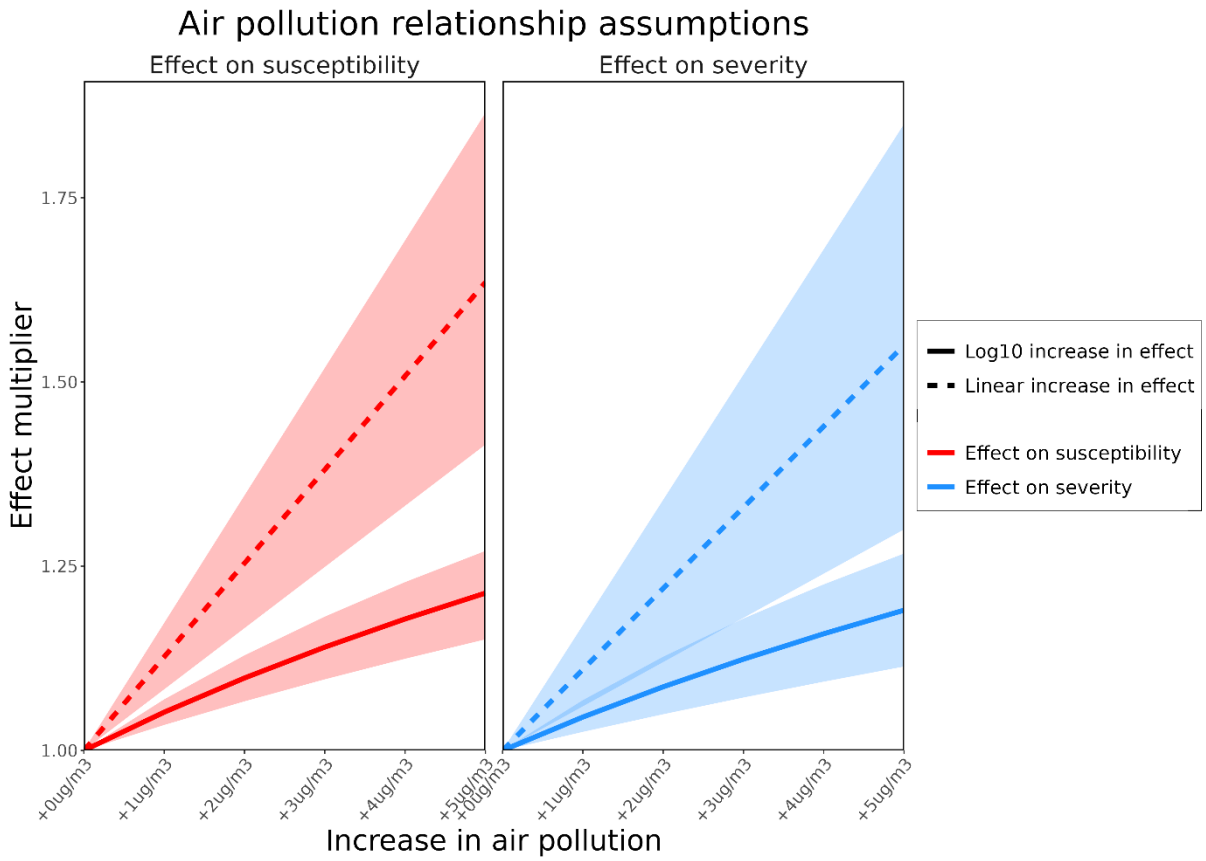


**Figure S9.** Effect multiplier as $PM_{2.5}$ increases. Exposure to the $PM_{2.5}$ (particulate matter ≤2.5 microns in diameter) air pollutant was modelled to have a 13% [95% CI 8–17%] increased effect on susceptibility to SARS-CoV-2 infection (19) (left panel) or an 11% [95% CI 6–17%] increased effect on COVID-19 severity (20) (right panel) per unit increase in exposure (0 to 5 μg/m$^3$) with a $\log_{10}$ (solid curves) or linear (dashed curves) increase in effect. Uncertainty is shown in shaded areas around the curves.

## 7. Supplementary figures

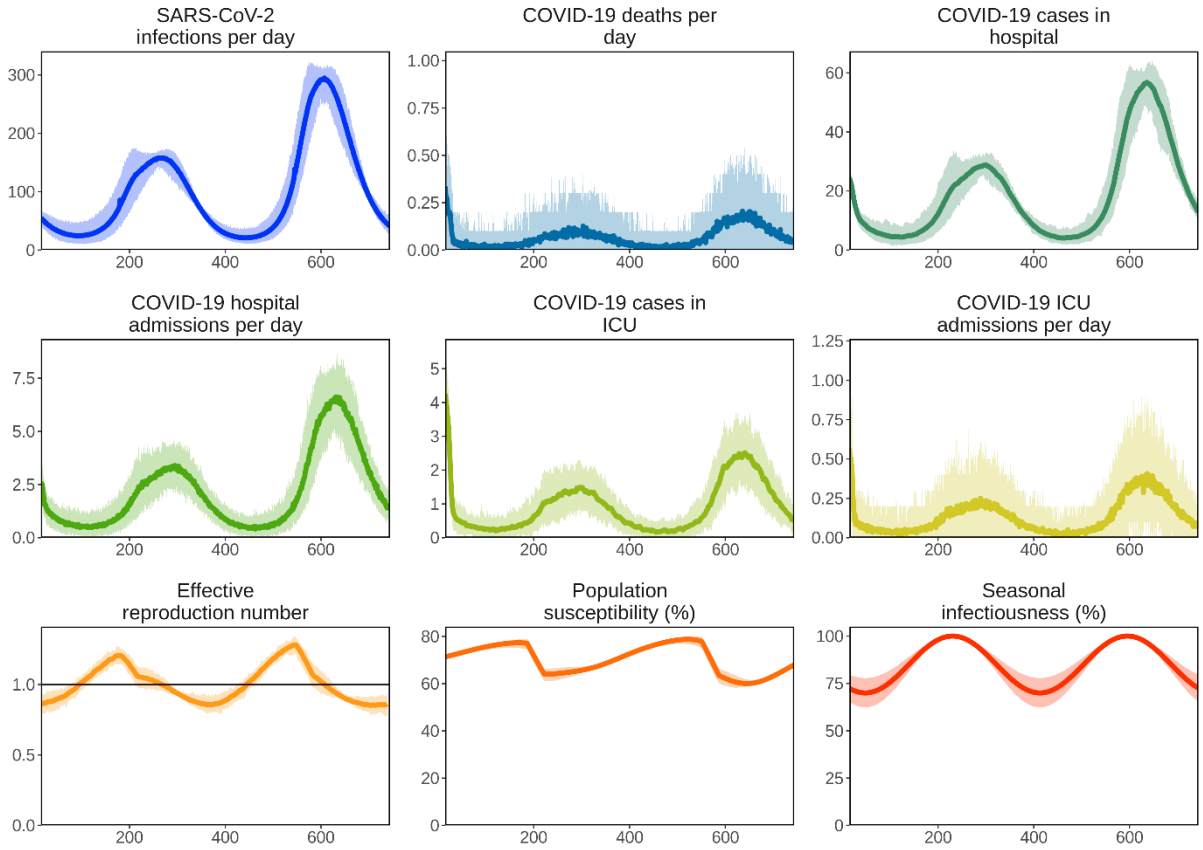


**Figure S10.** Baseline model metrics. The daily projected baseline model metrics with no increase in exposure to $PM_{2.5}$ (particulate matter ≤2.5 microns in diameter).

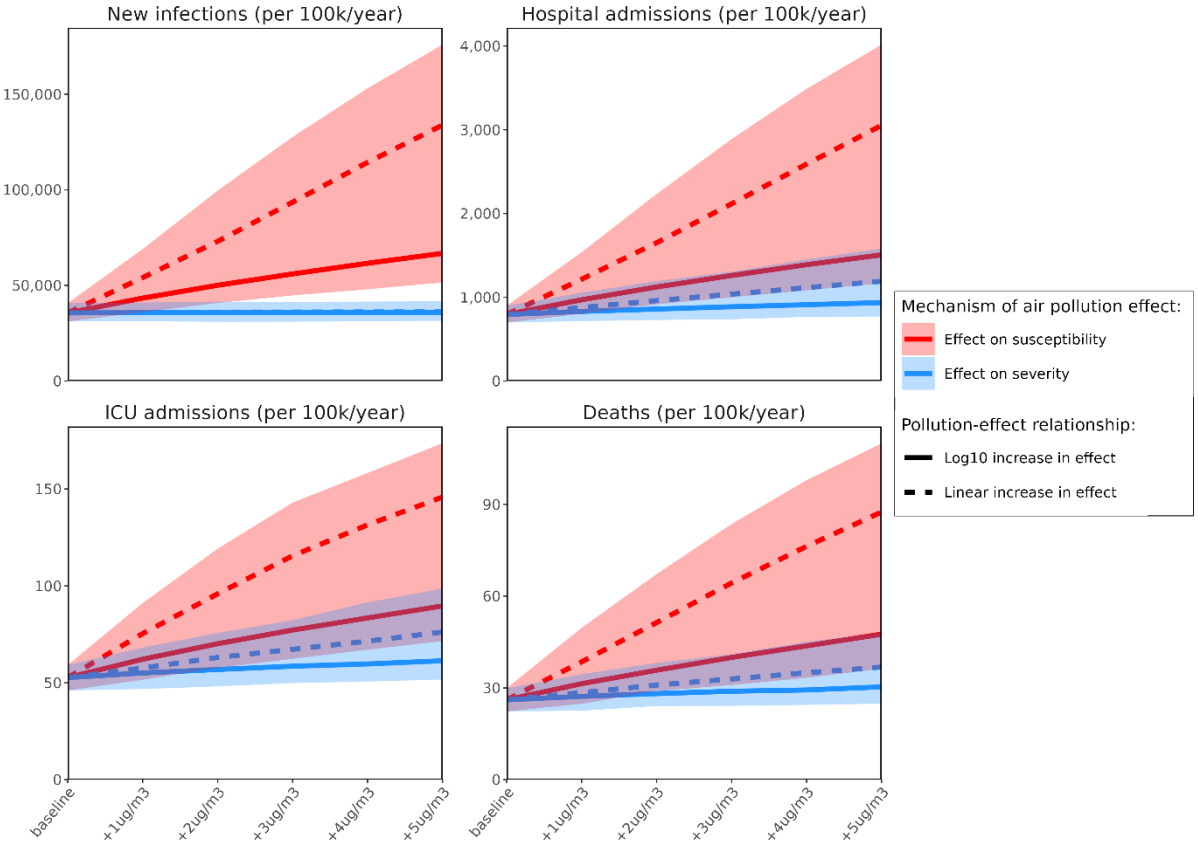


**Figure S11. a**. Projected COVID-19 health outcomes as $PM_{2.5}$ increases. The effect incrementally increasing exposure to $PM_{2.5}$ (particulate matter ≤2.5 microns in diameter)(+1–5μg/m$^3$) on new SARS-CoV-2 infections (top left panel, as shown in main text Figure 2), COVID-19 hospital admissions (top right panel, as shown in main text Figure 2), COVID-19 ICU admissions (bottom left panel), and COVID-19 deaths (bottom right panel) per 100,000 people per year with either a $\log_{10}$ (solid curves) or linear (dashed curves) increase in $PM_{2.5}$ exposure effect on susceptibility to SARS-CoV-2 infection (red curves, assuming a 13% [95% CI 8–17%] increase in effect per unit increase in exposure (19)) or COVID-19 severity (blue curves, assuming a 11% [95% CI 6–17%] increase in effect per unit increase in exposure (20)). Uncertainty and differences are shown in shaded areas between the curve pairs (red shading for susceptibility and blue shading for severity).

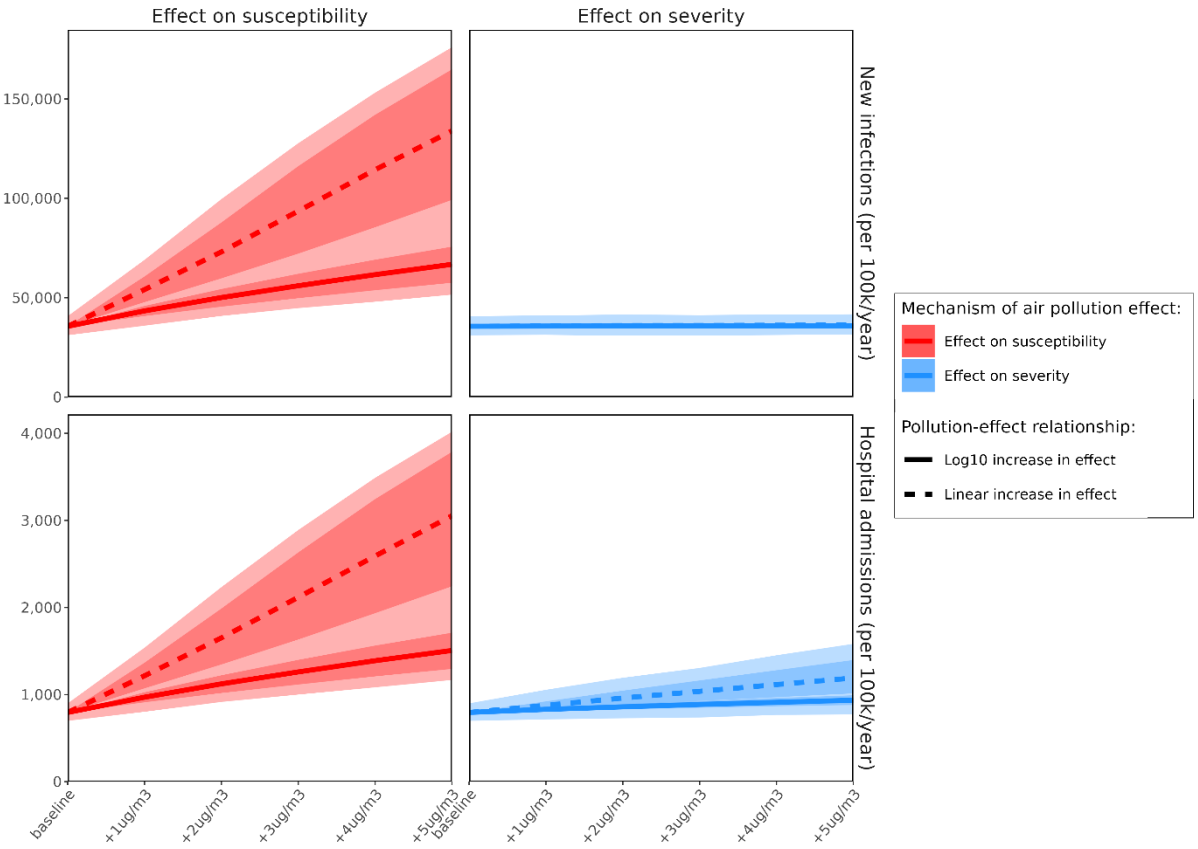


**Figure S11. b**. New SARS-CoV-2 infections and COVID-19 hospital admissions as $PM_{2.5}$ increases illustrated separately by effect of susceptibility and effect on severity. The effect incrementally increasing exposure to PM2.5 (particulate matter ≤2.5 microns in diameter) (+1–5µg/m3) on new SARS-CoV-2 infections (top row) and COVID-19 hospital admissions (bottom row) per 100,000 people per year with either a log10 (solid curves) or linear (dashed curves) increase in PM2.5 exposure effect on susceptibility to SARS-CoV-2 infection (red curves; assuming a 13% [95% CI 8–17%] increase in effect per unit increase in exposure (19)) or COVID-19 severity (blue curves; assuming a 11% [95% CI 6–17%] increase in effect per unit increase in exposure (20)). Uncertainty attributed to the best estimate for increase in effect is shown in the dark red shaded areas for susceptibility and dark blue areas for severity. Uncertainty attributed to the upper and lower bounds for increase in effect is shown in the light red shaded areas for susceptibility and light blue areas for severity, as well as the differences between the curve pairs.

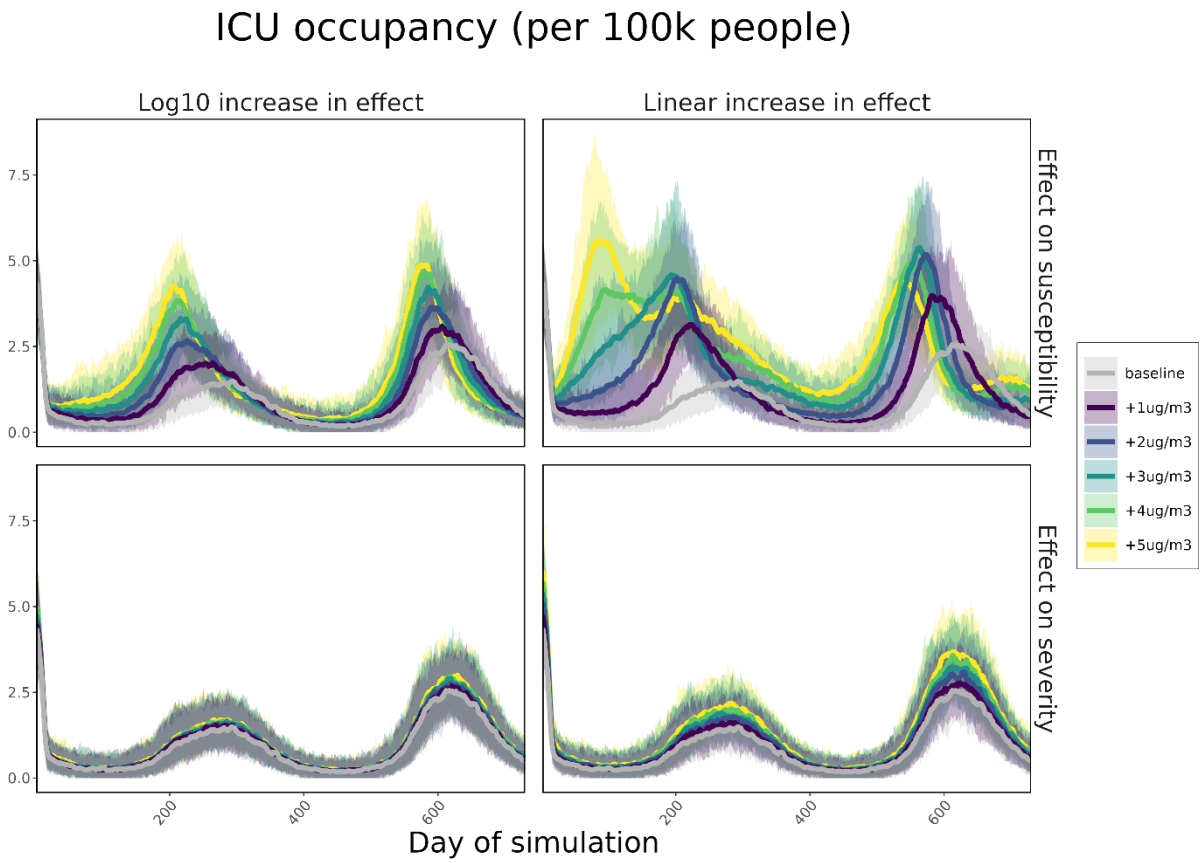


**Figure S12.** Daily ICU occupancy per 100,000 over time as $PM_{2.5}$ increases. The daily projected impact of incremental increases of exposure to $PM_{2.5}$ (particulate matter ≤2.5 microns in diameter) (+1–5μg/m$^3$) on ICU occupancy per 100,000 people over a two-year period assuming a $\log_{10}$ (left panels) or linear (right panels) increase in effect of exposure on susceptibility to infection (top row) or COVID-19 severity (bottom row) compared with a no exposure increase baseline (grey curves). Uncertainty shown in the shaded areas around the curves.

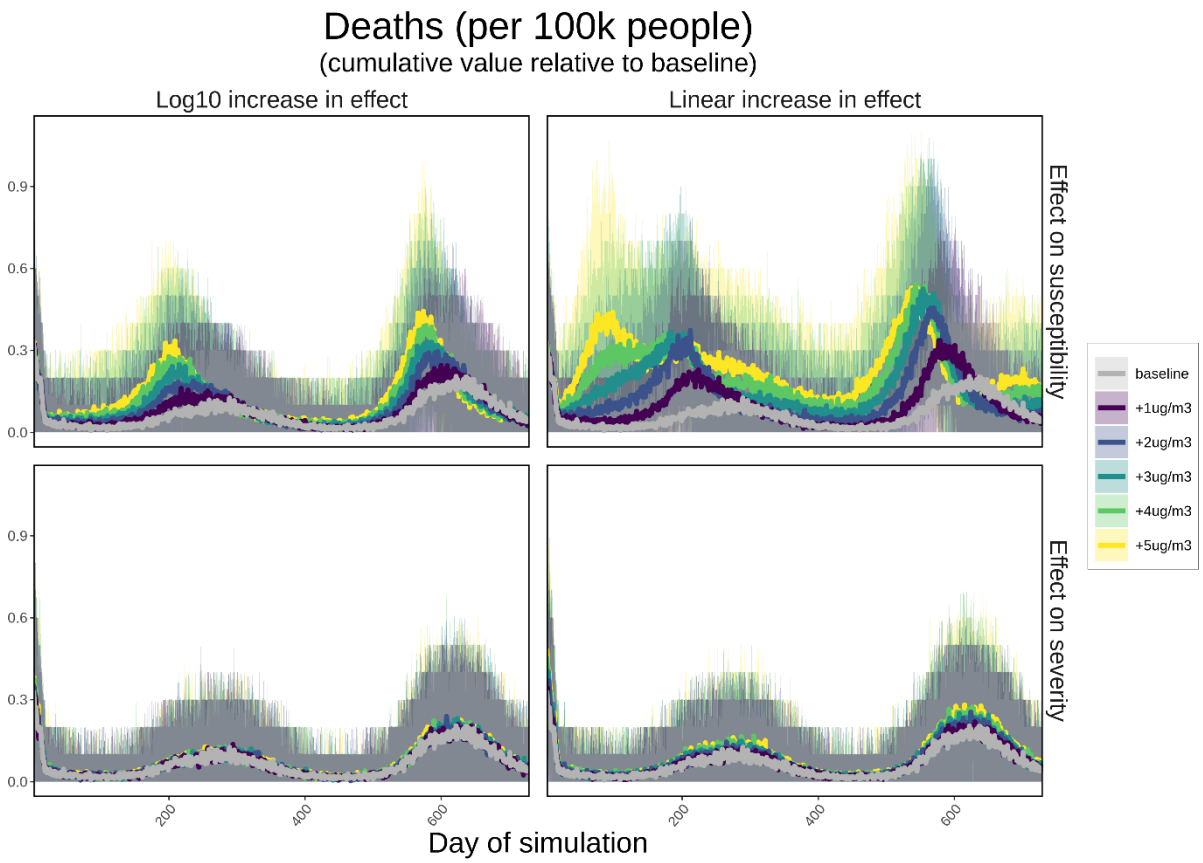


**Figure S13.** Daily COVID-19 deaths per 100,000 over time as $PM_{2.5}$ increases. The daily projected impact of incremental increases in exposure to $PM_{2.5}$ (particulate matter ≤2.5 microns in diameter) (+1–5μg/m$^3$) on COVID-19 deaths per 100,000 people over a two-year period assuming a $\log_{10}$ (left panels) or linear (right panels) increase in effect of exposure on susceptibility to infection (top row) or COVID-19 severity (bottom row) compared with a no exposure increase baseline (grey curves). Uncertainty shown in the shaded areas around the curves.

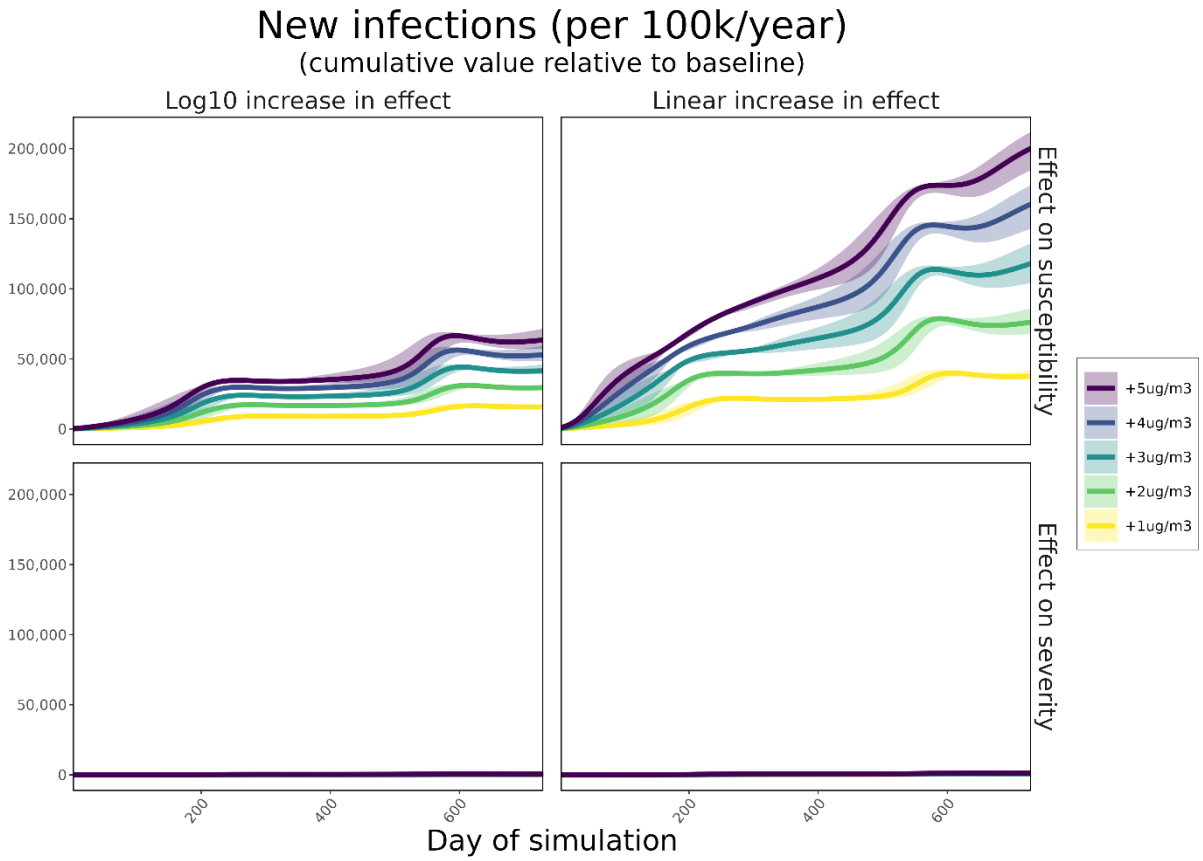


**Figure S14.** Cumulative SARS-CoV-2 infections per 100,000 as $PM_{2.5}$ increases. The cumulative impact of incremental increases in exposure to $PM_{2.5}$ (particulate matter ≤2.5 microns in diameter) (+1–5μg/m$^3$) on new SARS-CoV-2 infections per 100,000 people per year relative to baseline simulated with either a $\log_{10}$ (left panels) or linear (right panels) increase in effect of exposure on susceptibility to infection (top row) or COVID-19 severity (bottom row). Uncertainty shown in the shaded areas around the curves.

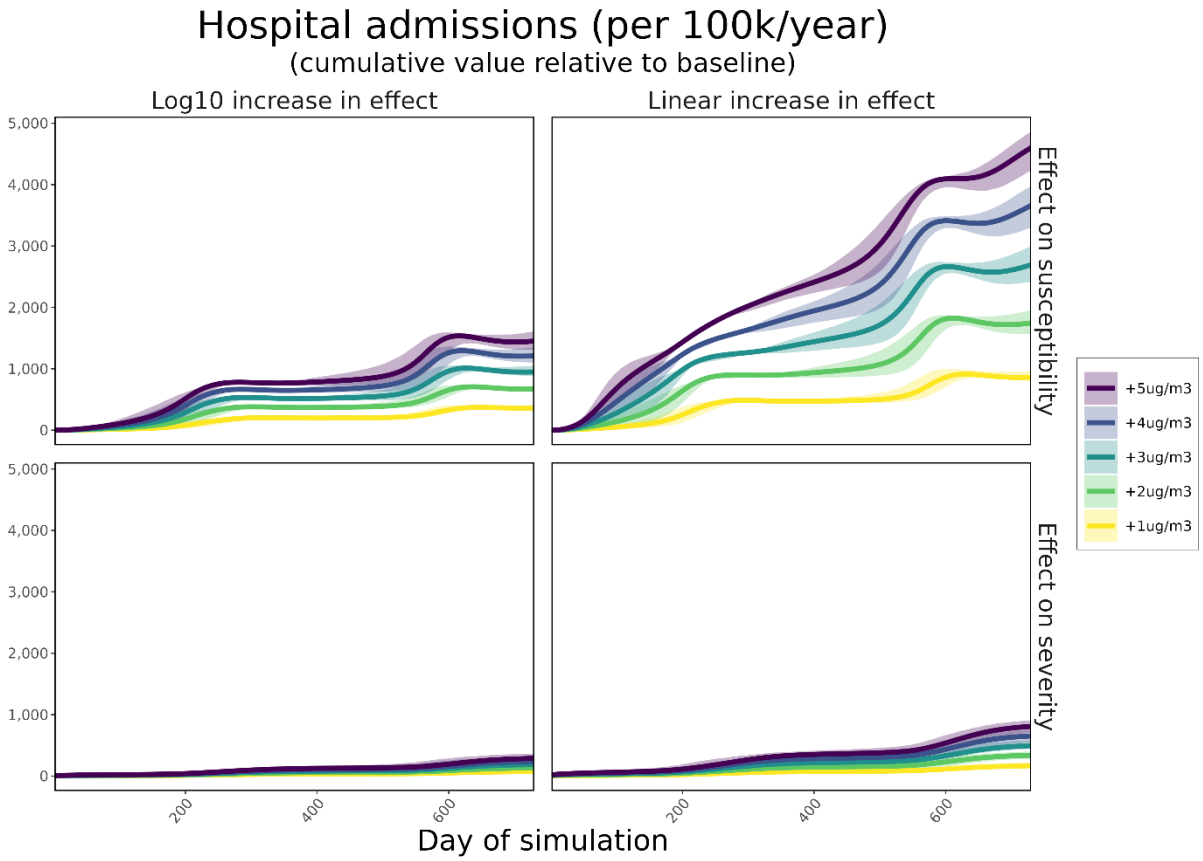


**Figure S15.** Cumulative COVID-19 hospital admissions per 100,000 as $PM_{2.5}$ increases. The cumulative impact of incremental increases in exposure to $PM_{2.5}$ (particulate matter ≤2.5 microns in diameter) (+1–5μg/m$^3$) on COVID-19 hospital admissions per 100,000 people per year relative to baseline over a two-year period assuming a $\log_{10}$ (left panels) or linear (right panels) increase in effect of exposure on susceptibility to infection (top row) or COVID-19 severity (bottom row). Uncertainty shown in the shaded areas around the curves.

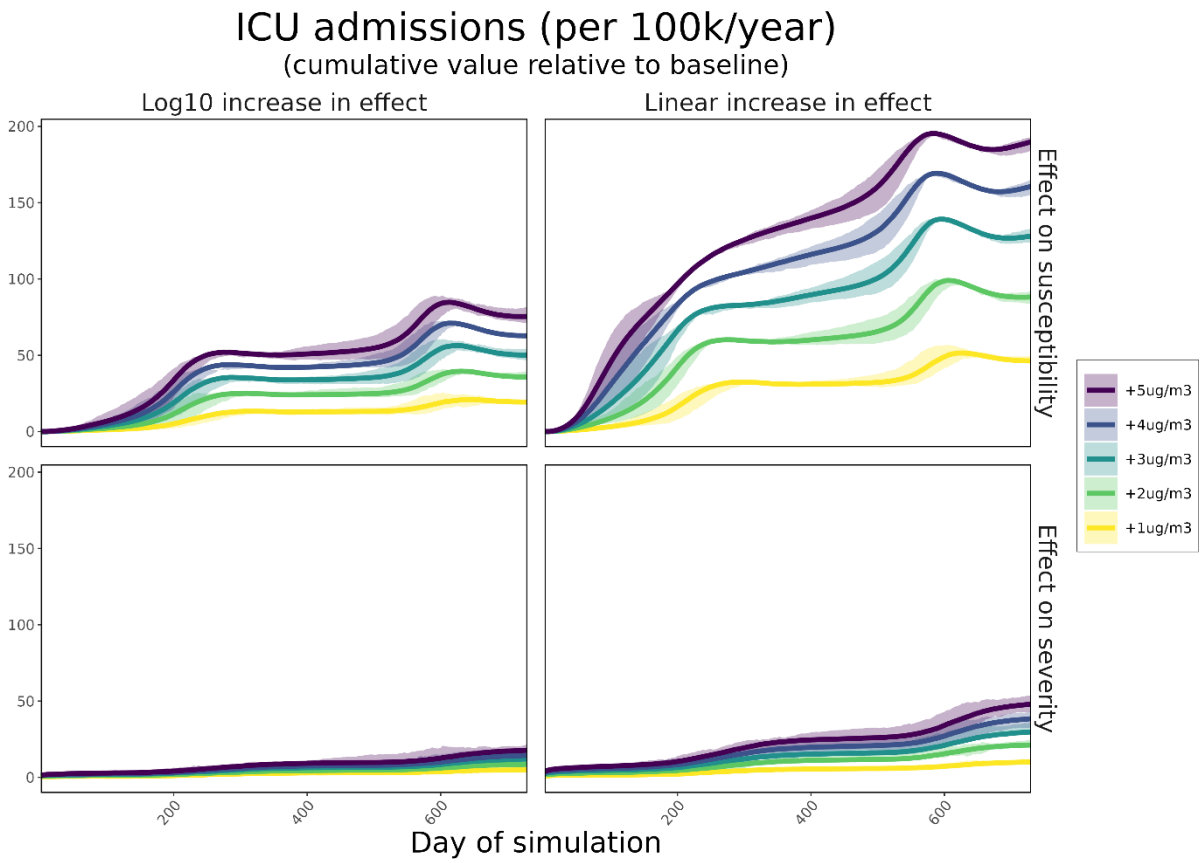


**Figure S16.** Cumulative COVID-19 ICU admissions per 100,000 as $PM_{2.5}$ increases. The cumulative impact of incremental increases in exposure to $PM_{2.5}$ (particulate matter ≤2.5 microns in diameter) (+1–5μg/m$^3$) on COVID-19 ICU admissions per 100,000 people per year relative to baseline over a two-year period assuming a $\log_{10}$ (left panels) or linear (right panels) increase in effect of exposure on susceptibility to infection (top row) or COVID-19 severity (bottom row). Uncertainty shown in the shaded areas around the curves.

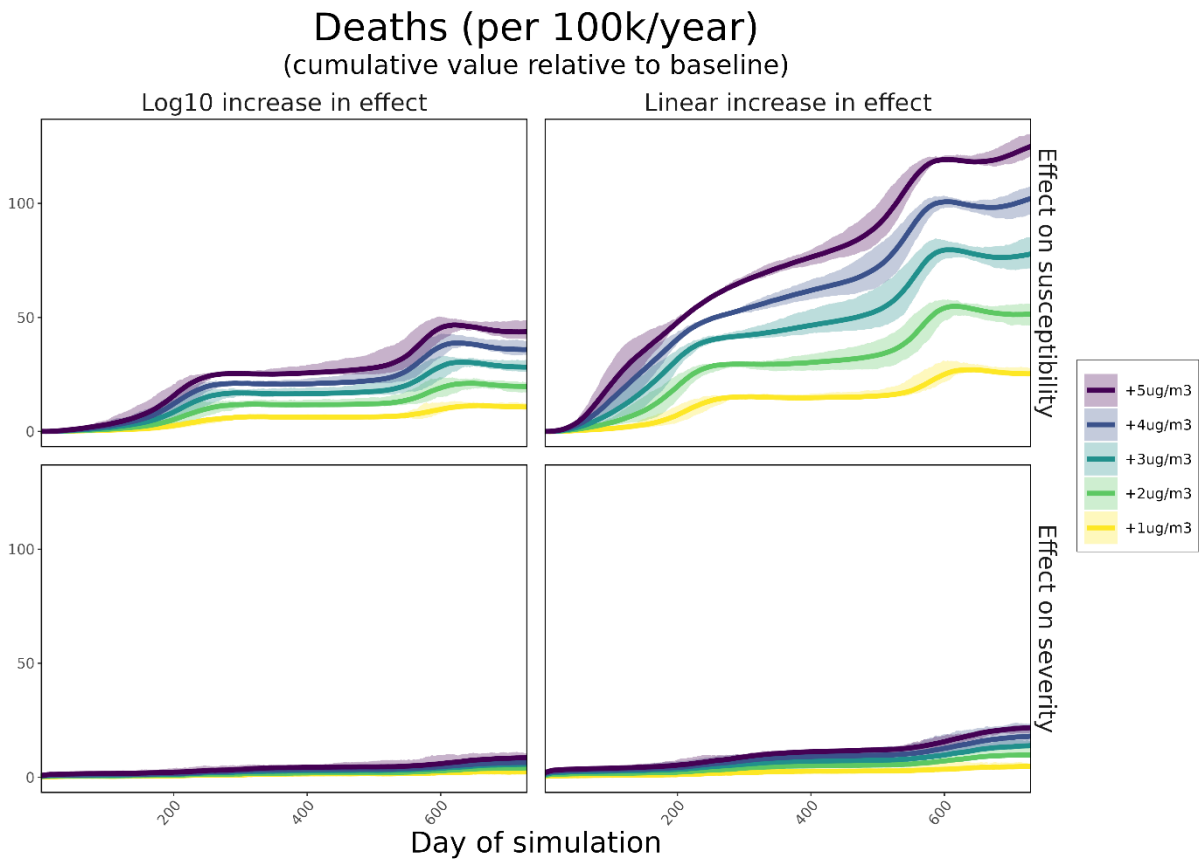


**Figure S17.** Cumulative COVID-19 deaths per 100,000 as $PM_{2.5}$ increases. The cumulative impact of incremental increases in exposure to $PM_{2.5}$ (particulate matter ≤2.5 microns in diameter) (+1–5μg/$m^3$) on COVID-19 deaths per 100,000 people per year relative to baseline over a two-year period assuming a $\log_{10}$ (left panels) or linear (right panels) increase in effect of exposure on susceptibility to infection (top row) or COVID-19 severity (bottom row). Uncertainty shown in the shaded areas around the curves.

## References


1. R: A language and Environment for Statistical Computing. R Foundation for Statistical Computing. Availabe online: https://www.R-project.org/ (accessed on 14 March 2023).
2. Jones, T.C.; Biele, G.; Mühlemann, B.; Veith, T.; Schneider, J.; Beheim-Schwarzbach, J.; Bleicker, T.; Tesch, J.; Schmidt, M.L.; Sander, L.E.; et al. Estimating infectiousness throughout SARS-CoV-2 infection course. *Science* **2021**, *373*, eabi5273. https://doi.org/10.1126/science.abi5273.
3. Lehtinen, S.; Ashcroft, P.; Bonhoeffer, S. On the relationship between serial interval, infectiousness profile and generation time. *J. R. Soc. Interface* **2021**, *18*, 20200756. https://doi.org/10.1098/rsif.2020.0756.
4. Kissler, S.M.; Fauver, J.R.; Mack, C.; Olesen, S.W.; Tai, C.; Shiue, K.Y.; Kalinich, C.C.; Jednak, S.; Ott, I.M.; Vogels, C.B.F.; et al. Viral dynamics of acute SARS-CoV-2 infection and applications to diagnostic and public health strategies. *PLoS Biol.* **2021**, *19*, e3001333. https://doi.org/10.1371/journal.pbio.3001333.
5. Khoury, D.S.; Steain, M.; Triccas, J.A.; Sigal, A.; Davenport, M.P.; Cromer, D. A meta-analysis of Early Results to predict Vaccine efficacy against Omicron. *medRxiv* **2021**, medRxiv:21267748. https://doi.org/10.1101/2021.12.13.21267748.
6. Andrews, N.; Stowe, J.; Kirsebom, F.; Toffa, S.; Rickeard, T.; Gallagher, E.; Gower, C.; Kall, M.; Groves, N.; O'Connell, A.-M.; et al. Covid-19 Vaccine Effectiveness against the Omicron (B.1.1.529) Variant. *New Engl. J. Med.* **2022**, *386*, 1532–1546. https://doi.org/10.1056/NEJMoa2119451.
7. Chivese, T.; Matizanadzo, J.T.; Musa, O.A.H.; Hindy, G.; Furuya-Kanamori, L.; Islam, N.; Al-Shebly, R.; Shalaby, R.; Habibullah, M.; Al-Marwani, T.A.; et al. The prevalence of adaptive immunity to COVID-19 and reinfection after recovery – a comprehensive systematic review and meta-analysis. *Pathog. Glob. Health* **2022**, *116*, 269–281. https://doi.org/10.1080/20477724.2022.2029301.
8. CDC. Science Brief: SARS-CoV-2 Infection-Induced and Vaccine-Induced Immunity. Availabe online: https://www.cdc.gov/coronavirus/2019-ncov/science/sciencebriefs/vaccine-induced-immunity.html (accessed on 14 March 2023).
9. Shattock, A.J.; Le Rutte, E.A.; Dünner, R.P.; Sen, S.; Kelly, S.L.; Chitnis, N.; Penny, M.A. Impact of vaccination and non-pharmaceutical interventions on SARS-CoV-2 dynamics in Switzerland. *Epidemics* **2022**, *38*, 100535. https://doi.org/10.1016/j.epidem.2021.100535.
10. Verity, R.; Okell, L.C.; Dorigatti, I.; Winskill, P.; Whittaker, C.; Imai, N.; Cuomo-Dannenburg, G.; Thompson, H.; Walker, P.G.T.; Fu, H.; et al. Estimates of the severity of coronavirus disease 2019: a model-based analysis. *Lancet Infect. Dis.* **2020**, *20*, 669–677. https://doi.org/10.1016/s1473-3099(20)30243-7.
11. Ferguson, N.M.; Laydon, D.; Nedjati-Gilani, G.; Imai, N.; Ainslie, K.; Baguelin, M.; Bhatia, S.; Boonyasiri, A.; Cucunubá, Z.; Cuomo-Dannenburg, G.; et al. *Report 9: Impact of Non-Pharmaceutical Interventions (NPIs) to Reduce COVID-19 Mortality and Healthcare Demand*; Imperial College London: London, UK, 2020.
12. Lauring, A.S.; Tenforde, M.W.; Chappell, J.D.; Gaglani, M.; Ginde, A.A.; McNeal, T.; Ghamande, S.; Douin, D.J.; Talbot, H.K.; Casey, J.D.; et al. Clinical severity of, and effectiveness of mRNA vaccines against, covid-19 from omicron, delta, and alpha SARS-CoV-2 variants in the United States: prospective observational study. *BMJ* **2022**, *376*, e069761. https://doi.org/10.1136/bmj-2021-069761.
13. Edridge, A.W.D.; Kaczorowska, J.; Hoste, A.C.R.; Bakker, M.; Klein, M.; Loens, K.; Jebbink, M.F.; Matser, A.; Kinsella, C.M.; Rueda, P.; et al. Seasonal coronavirus protective immunity is short-lasting. *Nat. Med.* **2020**, *26*, 1691–1693. https://doi.org/10.1038/s41591-020-1083-1.
14. Good, M.F.; Hawkes, M.T. The Interaction of Natural and Vaccine-Induced Immunity with Social Distancing Predicts the Evolution of the COVID-19 Pandemic. *mBio* **2020**, *11*. https://doi.org/10.1128/mBio.02617-20.
15. Spellberg, B.; Nielsen, T.B.; Casadevall, A. Antibodies, Immunity, and COVID-19. *JAMA Intern Med* **2021**, *181*, 460–462. https://doi.org/10.1001/jamainternmed.2020.7986.
16. Gebhard, C.; Regitz-Zagrosek, V.; Neuhauser, H.K.; Morgan, R.; Klein, S.L. Impact of sex and gender on COVID-19 outcomes in Europe. *Biol. Sex Differ.* **2020**, *11*, 29. https://doi.org/10.1186/s13293-020-00304-9.
17. Mossong, J.; Hens, N.; Jit, M.; Beutels, P.; Auranen, K.; Mikolajczyk, R.; Massari, M.; Salmaso, S.; Tomba, G.S.; Wallinga, J.; et al. Social Contacts and Mixing Patterns Relevant to the Spread of Infectious Diseases. *PLoS Med.* **2008**, *5*, e74. https://doi.org/10.1371/journal.pmed.0050074.
18. Funk, S.; Willem, L.; Dunbar, M.B.-K.; Pearson, C.A.B.; Clifford, S.; Jarvis, C.; Robert, A.; Hens, N.; Coletti, P. socialmixr: Social Mixing Matrices for Infectious Disease Modelling. Availabe online: https://cran.r-project.org/web/packages/socialmixr/index.html (accessed on 14 March 2023).
19. Travaglio, M.; Yu, Y.; Popovic, R.; Selley, L.; Leal, N.S.; Martins, L.M. Links between air pollution and COVID-19 in England. *Environ. Pollut.* **2021**, *268*, 115859. https://doi.org/10.1016/j.envpol.2020.115859.
20. Wu, X.; Nethery, R.C.; Sabath, M.B.; Braun, D.; Dominici, F. Air pollution and COVID-19 mortality in the United States: Strengths and limitations of an ecological regression analysis. *Sci. Adv.* **2020**, *6*, eabd4049. https://doi.org/10.1126/sciadv.abd4049.